Image Cover Sheet

CA011103

CLASSIFICATION	SYSTEM NUMBER
UNCLASSIFIED	515755

TITLE

Preliminary analysis of Echo 2000 data

System Number:

Patron Number:

Requester:

Notes:

DSIS Use only:

Deliver to:

This page is left blank

This page is left blank

Copy No. 15

DEFENCE R&D DÉFENSE

PRELIMINARY ANALYSIS OF ECHO 2000 DATA

John A Fawcett
Ron Kessel
Terry Miller
Vincent Myers
Mark Rowsome

Defence R&D Canada
Technical Memorandum
DREA TM 2001-009
February 2001

National Defence Défense nationale

Canada

REPRODUCTION QUALITY NOTICE

This document is the best quality available. The copy furnished to DRDCIM contained pages that may have the following quality problems:

: Pages smaller or Larger than normal

: Pages with background colour or light coloured printing

: Pages with small type or poor printing; and or

: Pages with continuous tone material or colour photographs

Due to various output media available these conditions may or may not cause poor legibility in the hardcopy output you receive.

☒ If this block is checked, the copy furnished to DRDCIM contained pages with colour printing, that when reproduced in Black and White, may change detail of the original copy.

National Defence
Research and Development Branch

Défense nationale
Bureau de recherche et développement

DREA TM 2001-009

PRELIMINARY ANALYSIS OF ECHO 2000 DATA

John A. Fawcett
Ron Kessel
Terry Miller
Vincent Myers
Mark Rowsome

DEFENCE RESEARCH ESTABLISHMENT ATLANTIC
PO Box 1012, Dartmouth
Nova Scotia, Canada
B2Y 3Z7

Approved by _____
Ron H. Kuwahara, Head Electromagnetics Section

February 2001

TECHNICAL MEMORANDUM

Prepared by

Defence Research Establishment Atlantic

Centre de Recherches pour la Défense Atlantique

Canada

Author

John A. Fawcett, Ron Kessel, Terry Miller, Vincent Myers, Mark Rowsome

Approved by

Ron H. Kuwahara

Head Electromagnetics Section

Approved for release by

K. Foster

Chair DRP

Abstract

In this report some preliminary results from target scattering measurements made at the DREA barge in April 2000 are presented. Various targets were mounted on a pole at about 5m distance from a transducer/hydrophone arrangement. The transducer allowed for the generation of harmonic bursts in the 10-100 kHz range and the scattered signals received at the hydrophone were recorded. This data was collected for a plate, spheres, cylinders, and a rock for a variety of centre frequencies and azimuthal orientations of the targets. A very large amount of data was collected and it is not possible to give a comprehensive presentation of the data; instead an interesting sampling of some of the results of our analysis of the data are presented.

Résumé

Dans le présent rapport, on donne certains résultats préliminaires des mesures de la diffusion des signaux par la cible effectuées à la barge du CRDA en avril 2000. Diverses cibles étaient montées sur un poteau à environ 5 m d'un ensemble transducteur/hydrophone. Le transducteur assurait la production de rafales d'harmoniques dans la gamme de 10-100 kHz, et on a enregistré les signaux diffusés reçus par l'hydrophone. Ces données ont été collectées pour une plaque, des sphères, des cylindres et une roche pour une variété de fréquences centrales et d'orientations azimutales des cibles. On a collecté une très grande quantité de données, et il n'est pas possible d'en donner une présentation exhaustive; on présente plutôt des échantillons intéressants de certains résultats de l'analyse de ces données.

This page intentionally left blank.

Executive summary

Background:

The ability to classify detections in Mine-Countermeasures as manmade or non-manmade is very important. Otherwise, the time spent investigating detections can quickly become prohibitive. In sidescan sonar surveys, highlight and shadow is often used as a detection and rough classification method. However, there are still often boulders and other non-mine objects which could be classified as mine-like on the basis of highlight and shadow alone. Any additional classification information besides the traditional intensity information could prove very useful. In particular, in this paper, the use of the details in the reflection time series is examined. For example, the details of the timeseries for a pulse reflected from a shelled-cylinder should be different than that of a rock. In April, 2000 the MCM group at DREA recorded many time series for a variety of targets, frequencies, and aspect angles. This report presents some of the analysis results from this data set.

Principal Results:

It is shown in this report, that there is indeed a wealth of useful information contained within the details of the scattered time series from various targets. This information should be able to be used to distinguish, or, at least, help distinguish the various target types.

Future Research:

It is hope to record the scattered signals (the true time series) from common sidescan sonars, such as the Klein 100, 300, and 455-kHz transducers, for targets on the seabed to see if it is possible to extract useful scattering information and combine this information with the traditional spatial image that a sidescan sonar provides.

Sommaire

Contexte :

La capacité de classer les objets détectés dans la lutte contre les mines comme artificiels ou naturels est très importante. Autrement, le temps passé à faire enquête sur les détections serait vite exorbitant. Dans les sondages au sonar latéral, la région illuminée et l'ombre sont souvent utilisées comme moyens de détection et de classification grossière. Cependant, il y a quand même souvent des rochers et autres objets qui ne sont pas des mines qui pourraient être classés comme ressemblant à des mines si l'on ne se base que sur la région illuminée et l'ombre. Toute information de classification supplémentaire à part l'information d'intensité classique pourrait s'avérer très utile. En particulier, dans le présent article, on examine l'utilisation des détails de la série chronologique de réflexion. Par exemple, les détails de la série chronologique pour une impulsion réfléchie par un cylindre creux devraient être différents de ceux correspondant à une roche. En avril 2000, le groupe LCM au CRDA a enregistré de nombreuses séries chronologiques pour une variété de cibles, de fréquences et d'angles d'aspect. Le présent rapport donne certains des résultats de l'analyse de cet ensemble de données.

Principaux résultats :

Le présent rapport révèle que les détails des séries chronologiques de signaux diffusés par les diverses cibles comportent en effet un trésor d'information utile. On devrait pouvoir utiliser cette information pour distinguer ou, pour le moins, aider à distinguer les divers types de cibles.

Recherche future :

Nous espérons enregistrer à l'avenir les signaux diffusés (série chronologique réelle) venant de sonars latéraux courants, tels que les transducteurs Klein de 100, de 300 et de 455 kHz, pour des cibles sur le fond de la mer pour voir s'il est possible d'extraire de l'information utile des signaux diffusés et de combiner cette information à l'image spatiale classique produite par un sonar latéral.

Table of contents

List of figures

Acknowledgements

We gratefully acknowledge the help of Ron Cunningham (Pernix), David Lewis, David Doucette, and Yolande Bonin in our endeavours at the DREA barge.

This page intentionally left blank.

INTRODUCTION

In April, 2000 the Mine Countermeasures (MCM) group at DREA spent 3 weeks at the DREA barge recording the signals scattered off a variety of targets. This was done for a variety of frequencies (harmonic bursts centred at different frequencies) for the targets at various aspects and at different target/source distances. Some data was also collected to measure the horizontal beam pattern of a Klein 100-kHz transducer, and some data was collected with the Klein 5500 sonar. This latter data will not be analyzed in this report.

In an earlier report [1] Cotaras reported on target strength measurements (20-50 kHz) range made for a variety of targets at the DREA barge. The work described here is similar in implementation; however, the main emphasis in this present work is not with respect to scattering strengths but more the features of the scattered signal, in the time or frequency domains or as a function of azimuth which might be used to distinguish various targets.

This work is motivated by the fact that in many MCM sonar applications it is often possible to make many detections, but additional information is required over standard sonar images in many cases in order to classify the detections as man-made objects or false alarms. If one was able to measure the true scattered signal from the target (instead of the standard envelope amplitude) for a sufficient bandwidth or if one could measure the variation of the scattered signal as a function of aspect, then this additional information might be very useful in classifying the object. Various publications [for example, 2-4] have shown the potential usefullness of such an approach.

It is well known that the acoustic energy scattered from an elastic object (solid or shelled) can consist of energy other than the standard specular reflection (see, for example [5]). There are a variety of wave types which propagate circumferentially about the object; if the target has an interior, energy can propagate within the object and scatter off either the back face or some interior scatterer. If the target has sharp edges, corners, or scatterers such as bolts, eye hooks, etc energy will be scattered or diffracted from these. If the object has a rough surface there will be additional scattering from the roughness. In summary there are a variety of scattering details which could be exploited to help classify an object. Reference [4] uses a tomographic approach with the reflected intensity to reconstruct the general shape of the scattered and a detailed analysis of the signal to yield further information.

THE EXPERIMENTAL SETUP

The targets used in the scattering experiments were an aluminium plate, a steel shelled sphere, an aluminium cylinder (air and water-filled), a rock, syntatic foam sphere, and a retro-reflector. They will be described in more detail in their own section. For the first two experiments, the data was recorded to floppy disk from a HP oscilloscope; this proved to be a tedious procedure and the sampling rate of approximately 100 kHz was inadequate for the higher source frequencies (50 kHz and above). Ron Cunningham (Pernix), a contractor working on updating the hardware/software data acquisition systems at the barge wrote us a very nice data acquisition interface for recording directly to the McIntosh computer at the barge; this system was capable of sampling at 1MHz. With this new software, the recording process was made considerably easier and a large amount of recorded data was quickly generated. Unfortunately, the data for the aluminium plate and the steel-shelled sphere were collected using the oscilloscope system and are not as of good quality as the latter data.

The transducer used in the experiments was the Fitzgerald transducer which allowed us to vary the centre frequency of the harmonic bursts from about 10-100 kHz. The F-33 is circular in shape consisting of a inner array of piezoelectric ceramic elements and additional outer elements. Because of these two arrays the F33 is capable of covering a wide frequency range (more details can be found in Bobber [5]). This transducer was bolted to one of the stations at the DREA barge. In the first experiment with the plate, the source was at one station, the hydrophone at another, and the target suspended by ropes at the end of the barge. From the second experiment onwards, this geometry was changed. From the mounting flange for the Fitzgerald transducer, an aluminium boom, 2.94 m in length was bolted with a hydrophone mounted from a small piece of wood at the end of the boom. This hydrophone was positioned to be on-axis with the centre of the transducer beam. This transducer/hydrophone set up is shown below in Fig.1. Thus the incident pulse will first pass the hydrophone and then after a time equal to twice the travel time to the target from the hydrophone, the reflected pulse will arrive. The targets were suspended from a second station. Both the transducer and target depths were approximately 15 m in depth; this meant that multipath arrivals were not an issue for our experimental geometries. A schematic of the typical experimental set up is shown in Fig.2

A variety of methods were used to affix the target to the bottom of the plate on the end of the pole. It is desirable to have the target at some distance from the pole in the main beam of the source transducer, in order to avoid reflections from the pole itself. On the other hand, there can be significant tidal currents in Bedford Basin, so that, for example, a target suspended at the end of a rope will significantly move with respect to the beam of the source transducer (the nominal beamwidth is about 12 degrees for most of the measurements) and the travel times of the reflected energy (with respect to the incident pulse) of such a target will vary noticeably due to motion. Thus, in fact, most of the targets were mounted in a fairly rigid manner using wood or metal to the pole. Rubber matting was the often wrapped about the mounting to the pole to minimize the reflections. In one instance, we directly measured the response of the attaching plate with the matting wrapped about it (no target) and found the reflections to be relatively insignificant.

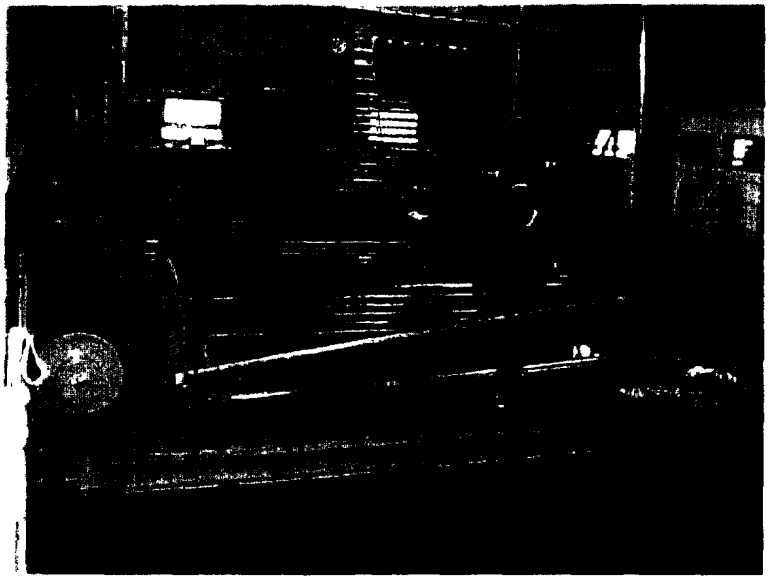

Figure 1 The hydrophone is at the end of the 2.94m long boom; in this picture the transducer is the Klein 100-kHz transducer

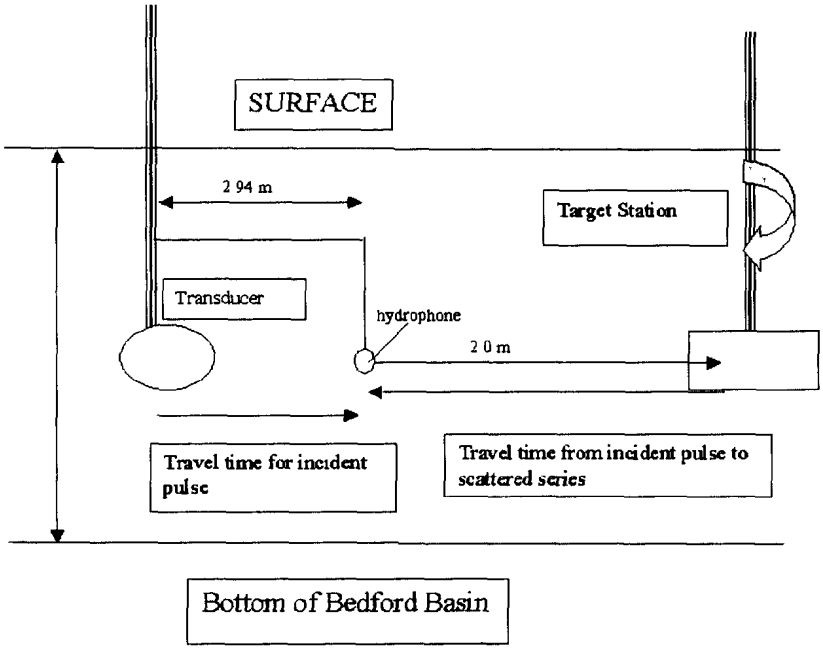

Figure 2 Schematic of source/target/hydrophone geometry

Figure 3 Setup with rock showing rubber matting wrapped around metal bar

THE TARGETS

Below, we describe some of the results from the individual targets: plate, sphere, cylinder, rock, syntatic foam sphere, and retro-reflector. Theses targets were simply chosen because they were readily available and covered a variety of shapes.

Aluminium plate

The first target considered was a 47 cm X 50 cm and 2 mm thick aluminium plate. The plate was suspended by two ropes from the upper corners of the plate to the side of the barge. The distance from the hydrophone to the plate was nominally 1.5m (definitely a near-field measurement!) . In this case the reflected signal is relatively strong (compared to what will be seen for other targets). In the plots below the signal for 20-30 kHz pulses are shown (Fig.4) in some detail and below that an ensemble of 40-80 kHz signals (Fig.5). By taking the ratio of the peak reflected energy to the incident pulse (the absolute values of the signal are smoothed), an estimate of the target strength can be obtained after accounting for the propagation distances. The results of this estimate are shown below in Fig.6, where it can be seen that the target strength has a significant frequency-dependence.

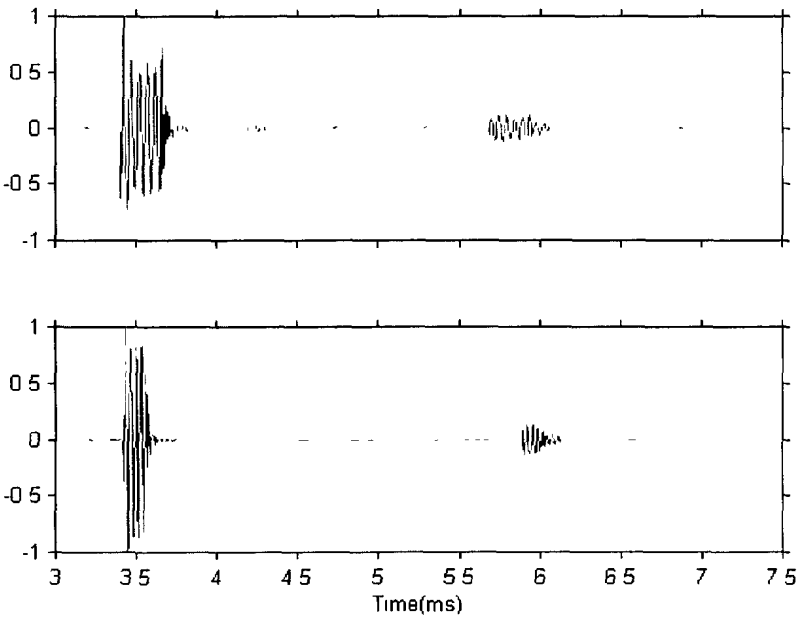

Figure 4 Incident and scatered signals from aluminium plate for 20 and 30-kHz pulse

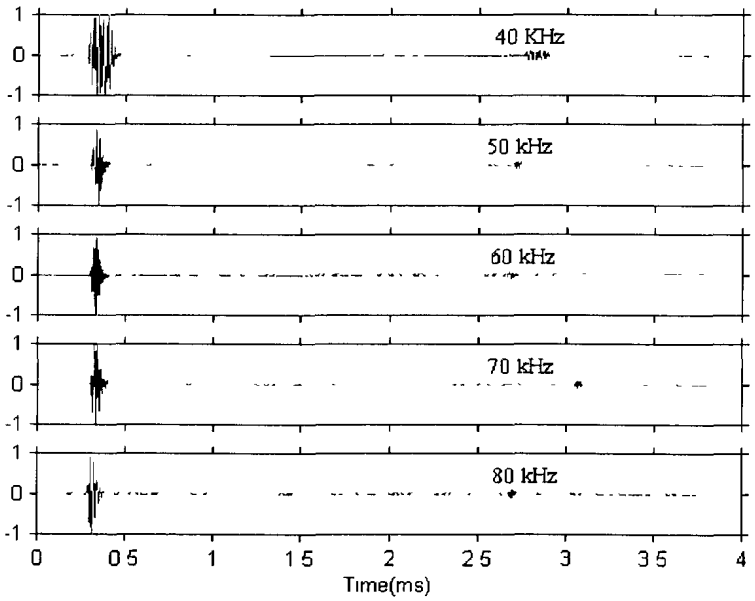

Figure 5 Representative pings for 40-80 kHz

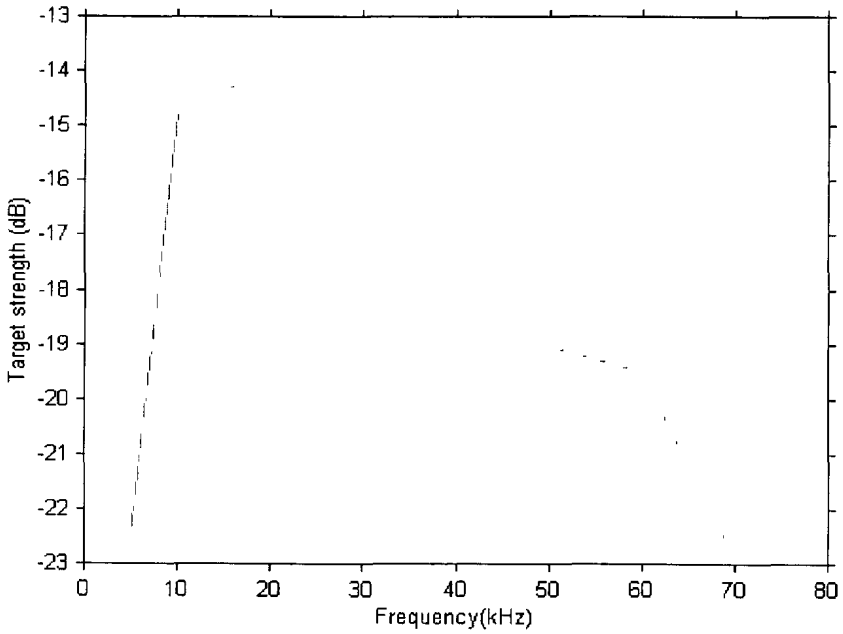

Figure 6 Frequency variation of target strength for plate

These values are much lower than the values from the standard flat-plate target strength formula which can be found in, for example, Urick[6] and are shown in Fig.7 (red curve). However, this formula is a far-field approximation and takes the plate to be a rigid reflector. Below we will derive a non-rigid, near-field expression.

Using the rigid Kirchhoff approximation, the target strength prediction would be

$$p^{sc} = \frac{1}{4\pi}\int_S 2ik\sin(\theta)\exp(ik\sqrt{R^2 + R'^2 - 2RR'\cos(\theta)})dS \qquad (1)$$

where S represents the surface of the plate, $k = 2\pi f/c$, f is frequency, c is sound speed, R is the range from the centre of the plate to the receiver, R' is the range to a point on the surface, and θ is the angle between these 2 positional vectors. In Eq.(1) we used that the incident field is normally incident on the plate, thus effectively being a constant over the plate. The angle θ is approximately equal to 90 degrees over the plate so that $\sin(\theta) = 1$ and $\cos(\theta)=0$. The square root factor then becomes

$$\sqrt{R^2 + R'^2 - 2RR'\cos(\theta)} = R + \frac{R'^2}{2R} \qquad (2)$$

with the resulting exponential phase expression,

$$\exp(\sqrt{R^2 + R'^2}) = \exp(ikR)\exp(ikR'^2/(2R)) \ . \qquad (3)$$

The second term in Eq.(3) is usually ignored, particularly when R is large. However, in the case of this experiment this factor is significant and cannot be ignored. Another important consideration is the reflection coefficient for the plate. In the Kirchhoff approximation of Eq.(1), the plate is taken to be rigid (i.e. reflection coefficient = 1). However, in reality we have a 2 cm thick plate surrounded on both sides by water. Thus, the effective reflection coefficient (accounting for reflections off the first and second plane of the plate and the multiple scattering within the plate) is frequency dependent. In fact, for low frequencies the effective reflection coefficient should tend to zero.

To approximately evaluate the integral of Eq.(1), we will approximate the plate (which is approximately a 50 x 50 cm square in this case) by a circle of radius 25 cm. Then we can write for the integral of the exponential phase-variation over this circle,

$$\int_0^{2\pi} \int_0^{L/2} \exp(ikR'^2/(2R))R'dR'd\theta = \frac{(\exp(ikL^2/(8R))-1)R}{2\pi ik} \tag{4}$$

Using this expression and the frequency-dependent reflection coefficient (the factor 2 in Eq.(1) is replaced by $2\Gamma(f)$), the resulting prediction for the target strength is shown in Fig.7(blue) with the corresponding standard prediction for a rigid square plate. The blue curve still predicts target strengths larger than the observed ones, but is in closer agreement than the standard formula and also has accurately modelled the frequency variation.

The reflection (Fig.8) from the plate is a somewhat extended version of the incident pulse. This becomes increasingly evident at higher frequencies and, in fact, two distinct arrivals start to become distinguishable. These secondary arrivals are most evident for the 50 and 60-kHz signals. The exact nature of these arrivals is unknown but could be due a wave propagating within the plate and scattering back off the edges of the plate.

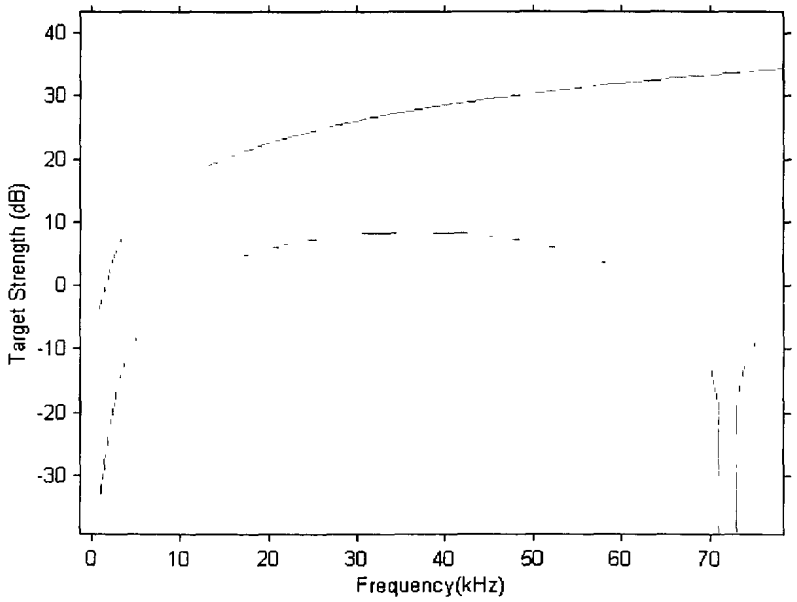

Figure 7 Modelled target strength for plate - red is standard flat plate formula, blue is near-field prediction

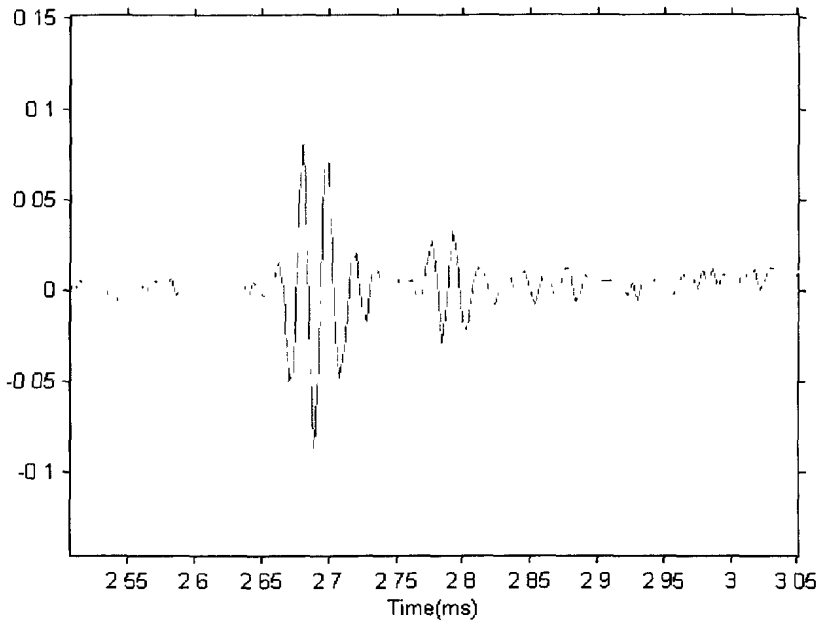

Figure 8 Reflected signal from plate at 60-kHz

Steel spherical scatterer

The sphere was approximately 0.25 m radius with a computed thickness of 2.7 mm. (this was computed by measuring the weight, assuming a density of 7.7 g/cm^3 multiplied by the computed surface area of the sphere). The front face of the sphere was located 4.15 m from the transducer and the transducer was 3.0 m from the hydrophone. Scattering from an elastic-shelled sphere can be modelled analytically using a harmonic series of Lengendre polynomial/radial Hankel functions [5] and the predicted backscattering strength of this sphere as a function of frequency is shown below. It can be seen from this spectrum in Fig.9 that there is enhanced backscattering (near the coincidence frequency) near 100 kHz. Unfortunately most of the energy in the neighbourhood of 100-kHz and higher is filtered out by the anti-aliasing filter which was employed during recording. It should be noted that even though cosine bursts of a certain frequency are used as the pulse, the pulses have a non-zero bandwidth due to their finite length of time. For example, a single-cycle burst will have a large bandwidth than a 2-cycle burst, etc.

In most of the signals recorded ranging from 5-kHz to 90-kHz pulses the backscattered signal consisted of the specular reflection and very little else which could be seen above the background noise. The one exception to this was at 50 kHz where up to 6 cycles of the input signal were used. In Fig.10 we show the resulting recorded signals using 1 and then 6 cycles of 50-kHz energy; in the second figure a secondary arrival can be seen. Unfortunately, if this pulse is modelled there is no such arrival predicted; however, this experimental sphere is, of course, not the perfect sphere used in the modelling and has protuberances and is, probably, of

somewhat uneven thickness, etc, so it may be that there is some feature causing this second arrival.

In Fig. 11 we show the empirically computed target strength. Here, the hydrophone- sphere distance has not been accounted for. At these near-field ranges it is not clear that a spherical spreading function is appropriate; accounting for this distance would increase the target strength slightly. Outside of a dip at 20 kHz, the target strength is approximately constant at –23 dB with respect to frequency. The predicted rigid sphere target strength is –18 dB for a sphere of this radius.

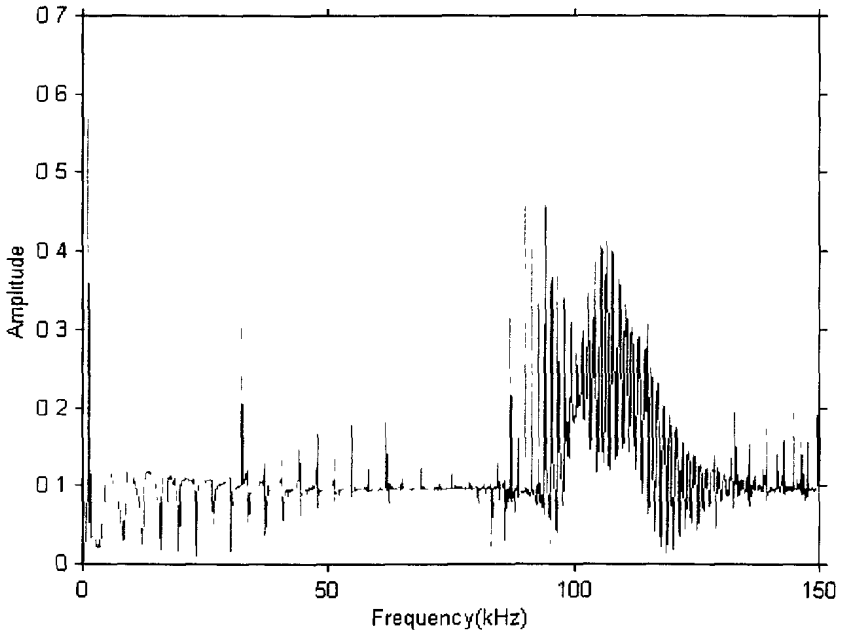

Figure 9 Predicted scattering strength as a function of frequency for steel-shelled sphere

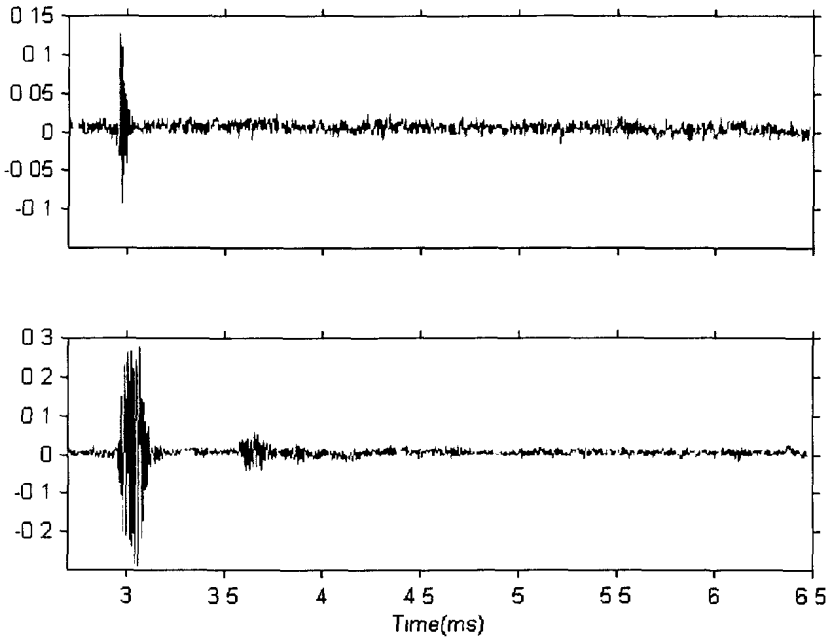

Figure 10 Reflected signals for 1 and 6 cycle 50-kHz pulses

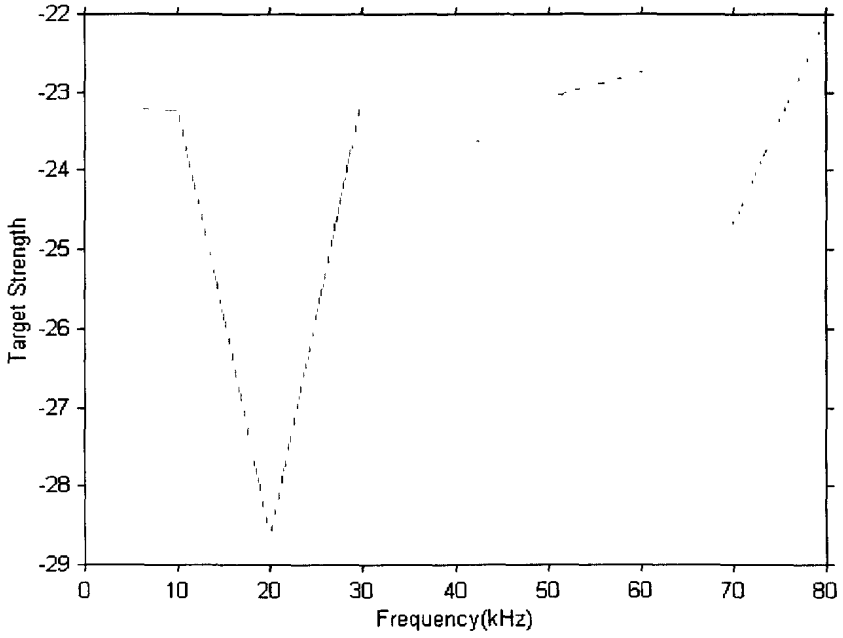

Figure 11 Experimental target strength of sphere

Aluminium Cylinder

The next target which was considered was an aluminium cylinder about 36 cm in length. The radius of the cylinder is approximately 14 cm with a thickness of about 2 cm. However, as can be seen below in Fig.12, the cylinder has significant flanges. The two flanges are not identical, so that the scattering response from the one end should be somewhat different than from the other end. In this case the scattering response was measured as a function of frequency and for different aspect angles. In Fig. 13 we show the amplitude of the scattered signal as a function of aspect angle at a centre frequency of 50 kHz. The source and hydrophone were fixed but the cylinder was rotated in 3 degree increments to generate the data shown below. The angles -90 and 90 degrees (or rotation increment 1 and 61) nominally correspond to end-on incidence and the values near the index 32 correspond to broadside incidence. However, as can be seen this is not exactly the case as one of the flat ends, in fact, corresponds to the index 5 and other end seems to be just starting to appear at index 61. This angular misalignment may be partly due to the fact that the tidal currents tended to twist the cylinder somewhat with respect to the beam. This misalignment is also manifested in the fact that the specular reflection in the scattering plot of Fig.13 is not symmetrical with respect to broadside. As one would expect, the strongest scattering occurs near the endcaps and broadside. However, significant scattering also occurs away from these angles and is associated with diffractions from the flanges and edges.

Besides the specular and diffraction scattering there are also the elastic effects. In particular, we can attempt to model the cylinder at the broadside aspect as an infinite, shelled cylinder for which there are analytic scattering solutions. Of course, in reality the cylinder used in the experiment is finite and has significant flanges at the ends. However, other studies with cylinders [2] have shown that the infinite cylinder model does a surprisingly good job for finite cylinders at the broadside aspect

Figure 12 Aluminium cylinder being filled with water

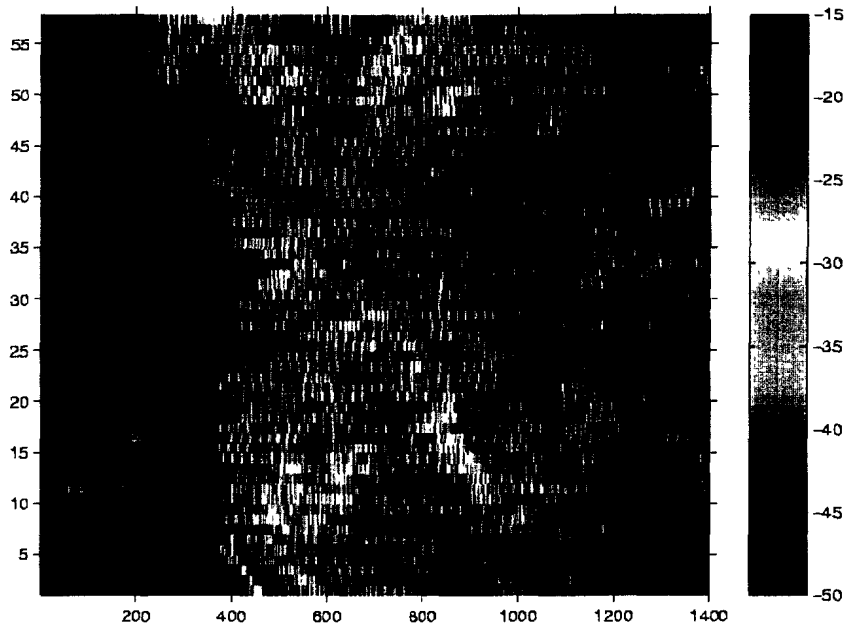

Figure 13 Time/azimuth amplitude(dB) of backscattered signal at 3 degree increments. Time index is in microseconds.

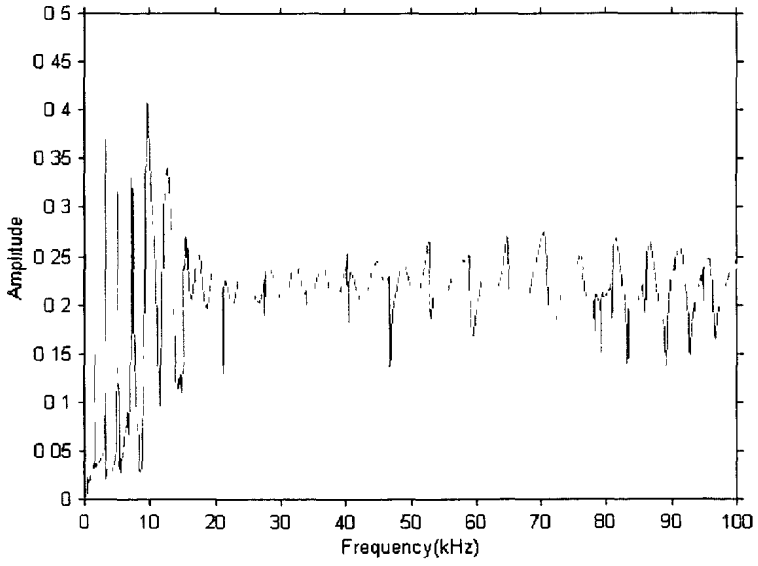

Figure 14 Theoretical (infinite cylinder) backscattered spectrum for an idealized shelled cylinder corresponding to the one of the experiment

It can be seen in the spetrum of Fig. 14 that there are strong resonances in the region 0-15 kHz. In the recorded data shown in Fig.15 it can be seen that the data for the 10-kHz tone burst does exhibit "ringing" after the initial specular reflection. This agrees well with the model time series constructed using the complex spectra and Fourier synthesis. In Fig.16 the time series, data and model, are shown for a 50-kHz pulse are shown. In this case the predicted amount of non-specular energy is small and this is, in fact, the case with the experimental data.

The cylinder was then recovered from the water, filled with water, and put back down to depth and the experimental procedures repeated. The resulting time/aspect data for a 50-kHz pulse is shown below in Fig.17. The data is somewhat nicer than for the air-filled case as the results are more symmetrical about broadside. The overall-structure is similar to the air-filled case; there is now a region of high-energy return centred at approximately angle-index 20 (or 60 degrees) from the bottom of Fig.17. This energy is not evident in the air-filled case. This is not as evident at the angle symmetrical about broadside, but recall that the cylinder's flanges are quite different at the 2 ends. Perhaps, this return corresponds to a raypath which propagates within the cylinder and reflects off the back end in some manner. In Fig.18 the computed spectrum for a water-filled infinite cylinder is shown; this spectrum is significantly more complicated "looking" than the one for the air-filled cylinder. This is because energy can now propagate within the cylinder and hence there are many more propagation paths possible. Once again the computed spectrum can be used to Fourier synthesize a pulse. In Figure 19 a comparison of the theoretical time series and the experimental time series for the water-filled cylinder at 30 kHz are shown. As can be seen there are significant non-specular arrivals which are, indeed, predicted by theory. Note that the experimental and modelled series are normalized such that the peak values agree. The 30-kHz pulse seems to be near-optimal for producing this non-specular response. A comparison of the time series for 30, 50, and 70-kHz pulses is shown in Fig.20. This behaviour is also predicted by theory as shown in Fig.21 (here the pulse length in time duration was kept the same)

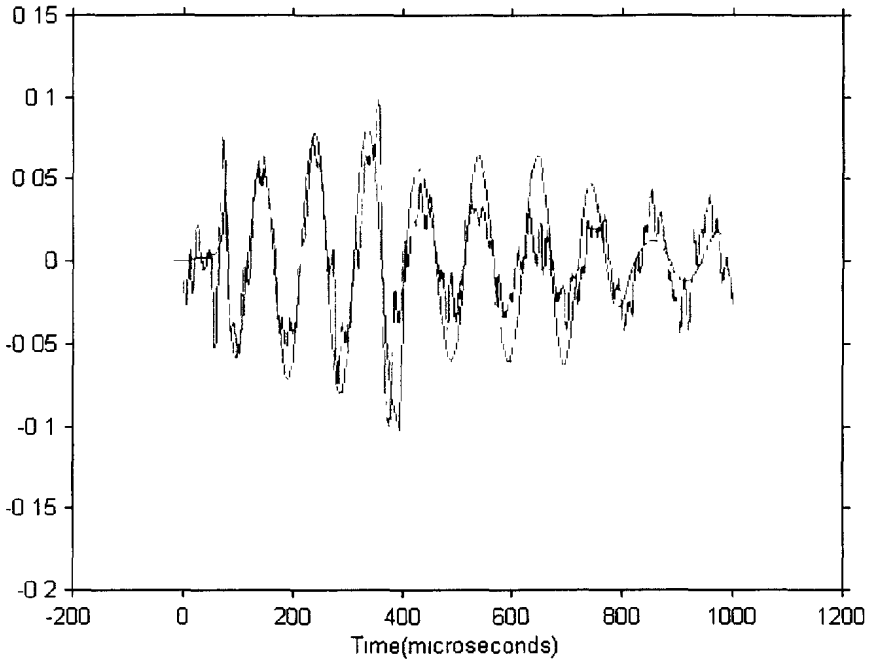

Figure 15 Segment of scattered time series at broadside for 10-kHz pulse showing experimental (blue) and modelled (red) time series. Note the significant ringing which takes place after the initial specular reflection (the first 3 1/2 oscillations)

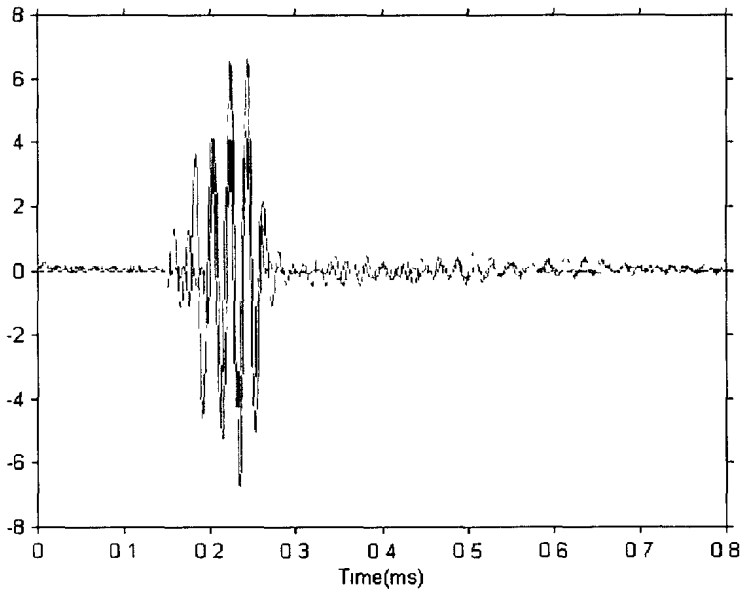

Figure 16 Scattered time series at broadside for 50-kHz pulse showing experimental (blue) and modelled (red) time series.

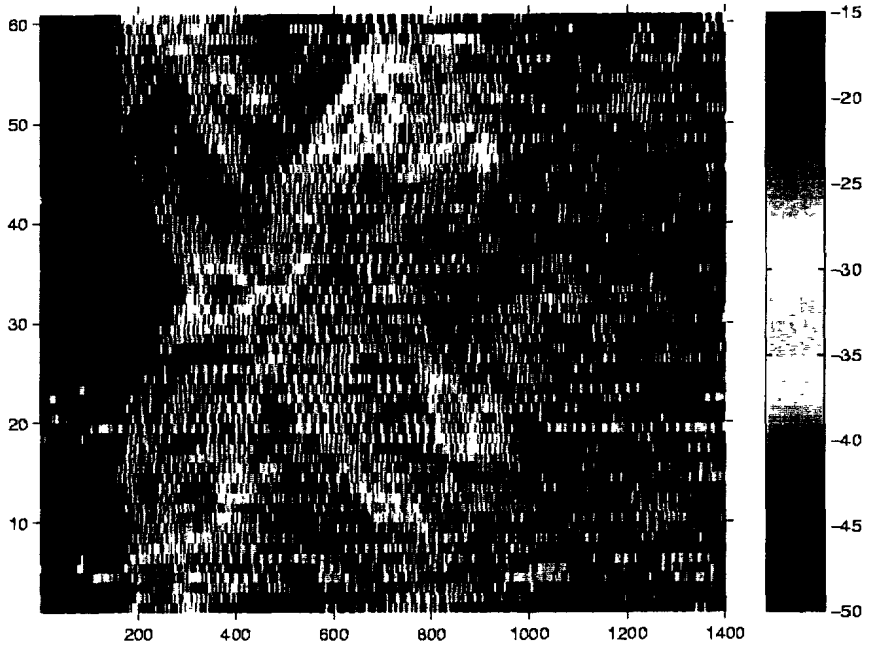

Figure 17 Time/aspect plot for water-filled cylinder at 50-kHz. Angle (y-axis) is in 3 degree increments and x-axis (time) is in microseconds

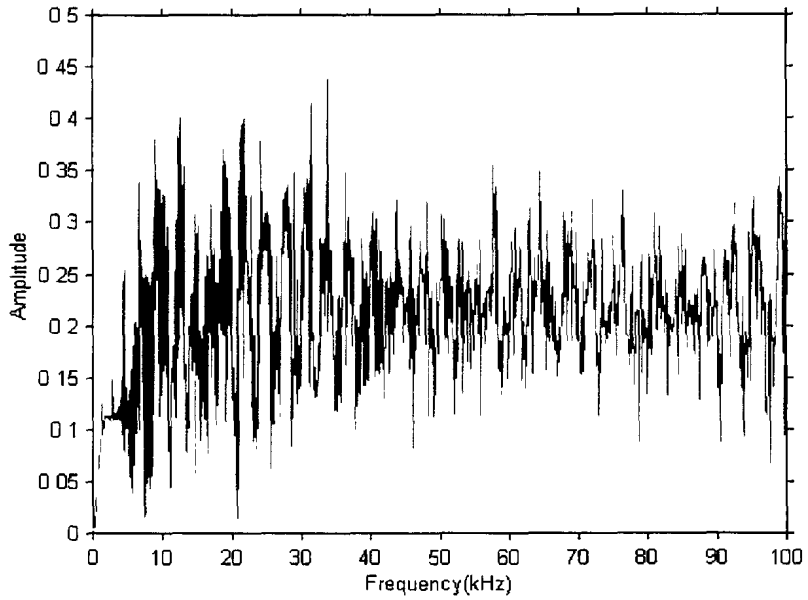

Figure 18 Theoretical (infinite water-filled cylinder) spectrum of backscattered signal

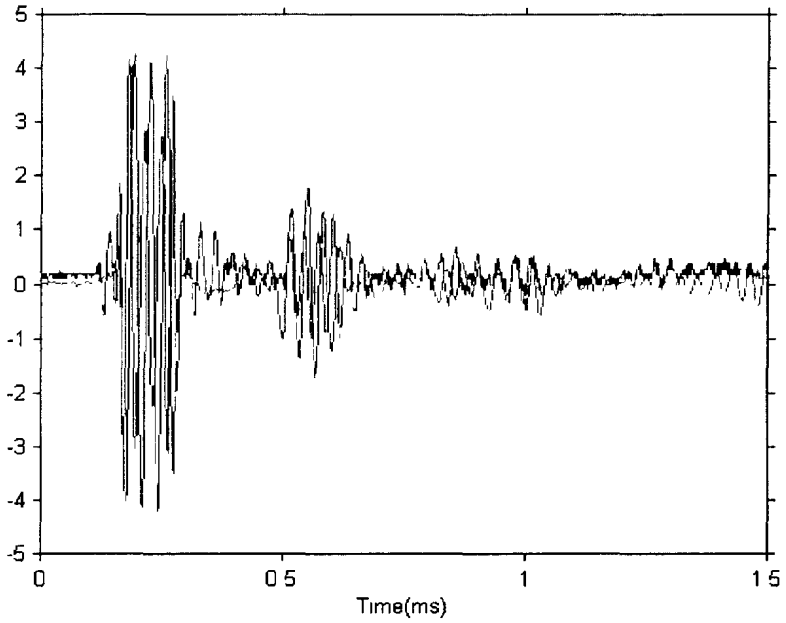

Figure 19 Experimental(blue) and modelled (red) time series for scattering from water-filled cylinder

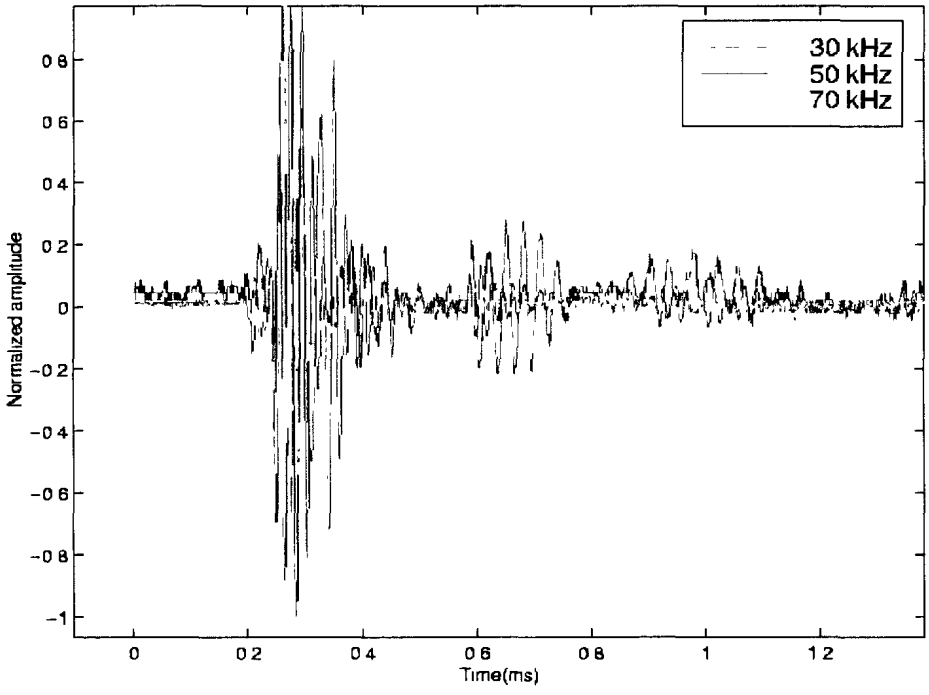

Figure 20 Variation of backscattered time series with pulse centre frequency

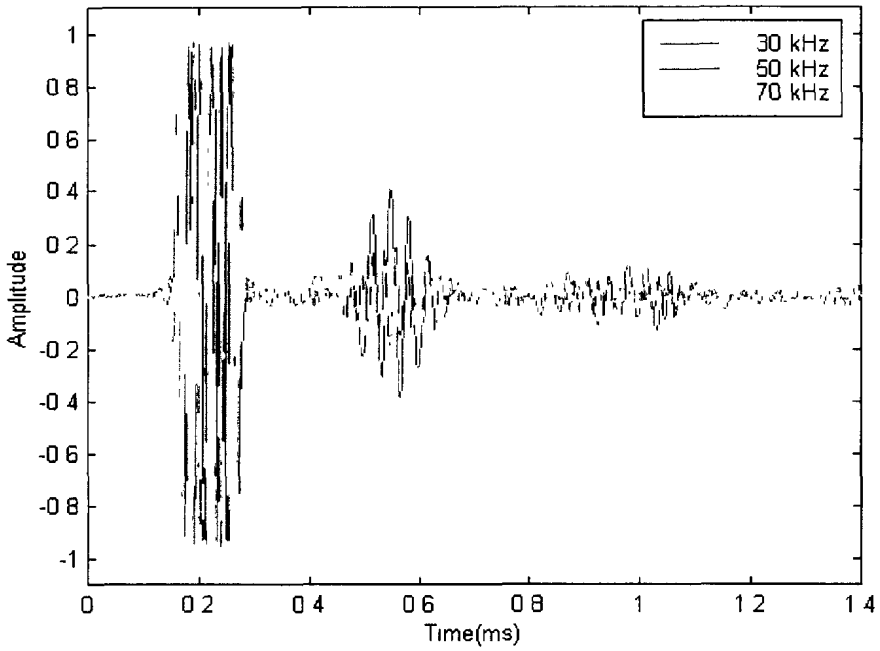

Figure 21 Modelled variation of time series with frequency

A Nova Scotia Rock

The next target we consider is a rock (Granite) which we obtained at random but which is typical of seabed debris. It is a rather angular, multi-faceted rock shown in Fig.22. It is hard to give dimensions for the rock, but its maximum length is about 30 cm. In Fig.23 the time/azimuth plot is given. In this case the rock was rotated a full 360 degrees. The time series are very complicated and instead of a few isolated events, it is more a continuum of scattering, with the arrivals from the various scattering locations of the rock overlapping each other. There is significant scattering at all aspect angles.

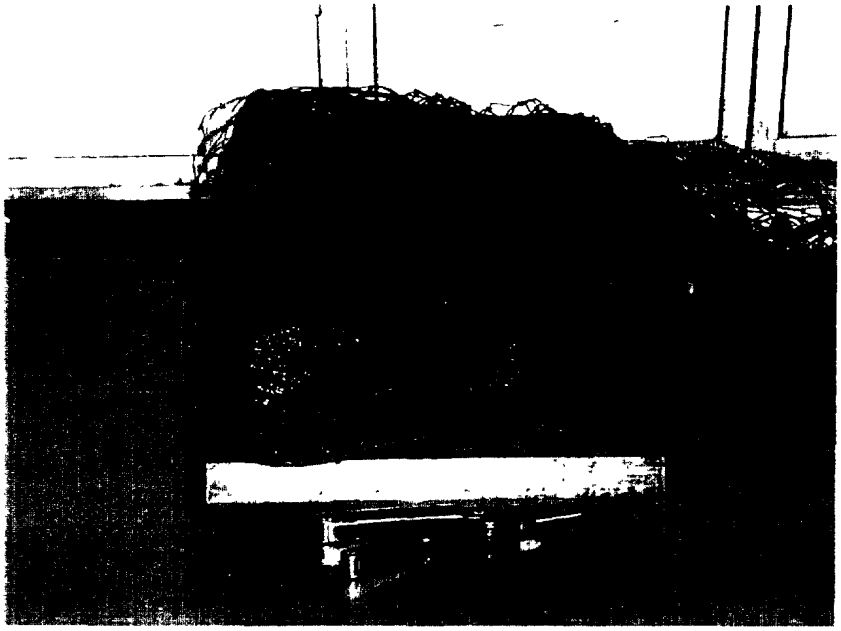

Figure 22 A rock; note the significant faces of the rock with additional facets on these faces.

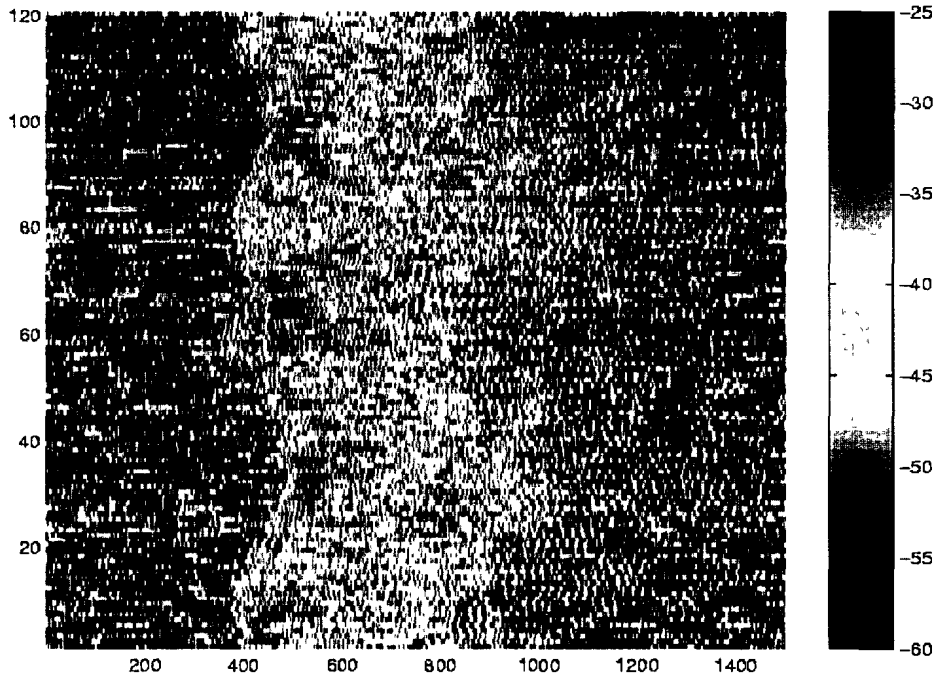

Figure 23 Time/aspect variation of scattering of 50-kHz pulse from rock

In Figure 24 we show the time series for 30, 50, and 70-kHz pulses (at a fixed number of cycles) at a fixed aspect angle. It should be noted that there may be some movement of the rock between pings so that it cannot be guaranteed that the time series correspond exactly to the same orientation of the rock. However, as one might expect, there seems to be a tendency for the higher frequencies to resolve individual features on the rock better.

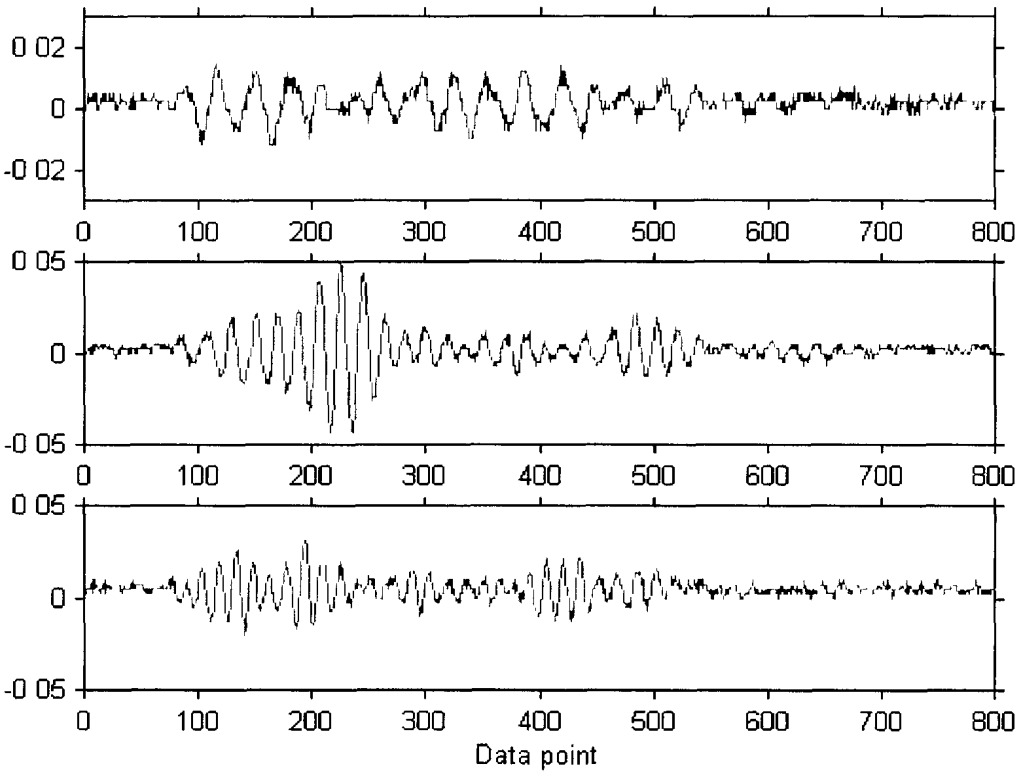

Figure 24 Frequency variation (30, 50 and 70 kHz) of backscattered signal (at fixed azimuth) from rock

Tomographic reconstruction of scatterer shape

From this trial there are three sets of data; the air-filled cylinder, the water-filled cylinder and the rock for which either 180 or 360-degree coverage was carried out. In the cases of the cylinder, it was thought that 180 degree coverage would suffice (and then the data could be simply "reflected" to produce a 360 degree set) as the cylinder is roughly symmetric about its axis. Unfortunately, especially in the air-filled cylinder case, the coverage did not cover both endcaps, so that the coverage is somewhat incomplete for backprojection methods. In retrospect, one should certainly do full 360 degree coverage even in cases where it may not be theoretically necessary.

In the following we attempt to use the scattering data to determine geometrically where the strong sources of scattering are [4]. In reality, the source/receiver location was fixed and the target was rotated in 3 degree increments. However, conceptually we can consider the target fixed and a sequence of source/receiver positions at 3 degree increments around the centre of the target. We will simplify the problem by ignoring the vertical variation of the target and consider only a two-dimensional projection of the target. Let us define the time variable as zero when the centre of the incident pulse passes the hydrophone. We will take the energy incident on the target to be approximately a plane wave, propagating in the direction defined by the radial from the hydrophone to the centre of the target. The target is discretized into a number of square patches and each patch is represented by the midpoint of the patch. Then for hydrophone position j (recall that we are considering the source/receiver to be at different angles) the two-way travel time for patch i can be written as

$$T(i,j) = \tau(i,j) + \kappa(i,j) \tag{5}$$

where the first term $\tau(i,j)$ represents the travel time of the incident plane wave to the patch i (i.e., we make the assumption that the incident pulse can be modelled as a plane wave incident upon the target; in fact, taking the incident wavefront to be spherical yields almost identical results) and the second term $\kappa(i,j)$ is the travel time for the scattered energy from patch i to hydrophone j. Then from the data matrix (the discrete time series for the various angular positions) we will sum for patch i all the data points which correspond to the travel times as defined above to determine a relative estimate of the reflectivity R_i. Instead of using the raw time series directly we use the envelope of the signal as the input data D and average this over 20 time points,

$$R_i = \sum_j D(T(i,j)) \tag{6}$$

This was done so that the intensities added up would be fairly smooth function of time, rather than summing up a very oscillatory function.

In Figs. 25 and 26 we show the resulting reconstructions for the rock and the water-filled cylinder. We do not show the air-filled cylinder; this did not work well at all. The reconstruction of the rock seems very reasonable. The reconstruction of the water-filled cylinder shows one of the sides of the cylinder and an indication of one of the endcaps. We expect that if a full 360 degree rotation had been done the reconstruction would have been much better. It can also be seen that some energy has been placed off the cylinder; this probably corresponds to some circumferential arrival, which does not correspond to a geometrical position on the cylinder.

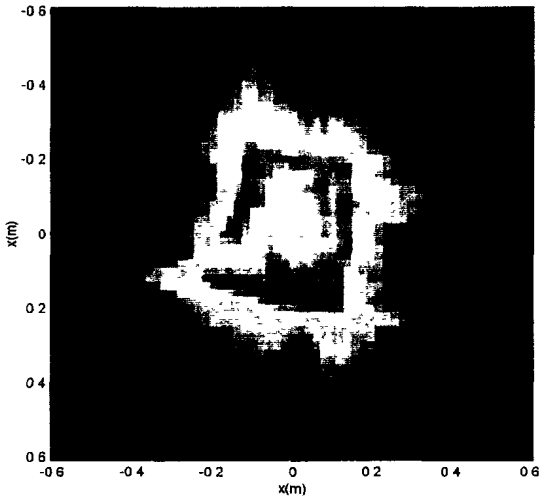

Figure 25 Reconstructed reflectivity of rock

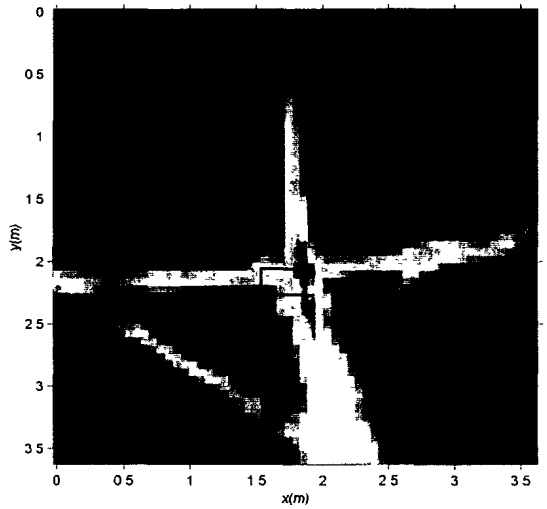

Figure 26 Reconstructed reflectivity of water-filled cylinder

Syntatic Foam Sphere

Syntatic foam is an epoxy/ glass bead composite. The details of the glass beads and their density vary according to the desired strength (or crush resistance) of the sphere. The syntatic foam we used had a diameter of 38 cm. In Fig.27 a representative 40-kHz backscattered signal is shown. The interesting feature is that there is a first reflection, presumably the specular reflection, and then a stronger event. The time between the 2 events is rather small; for example, if one hypothesizes that energy propagates within the sphere and scatters off the back face, this time difference would indicate an interior sound speed of approximately 3000 m/s which seems unlikely. If one hypothesizes a circumferential wave then the same conclusion of a high propagation speed is reached. Perhaps due to the composite nature of the interior material there is some complicated internal scattering mechanism taking place – this is an area of future research.

An experimental possibility considered was that one of the reflections was due to the plate or piece of wood to which the sphere was attached. In order to check this, we removed the sphere and measured the response of just the attachment gear; it was found that the scattering was relatively low and did not account for either of the 2 scattering events.

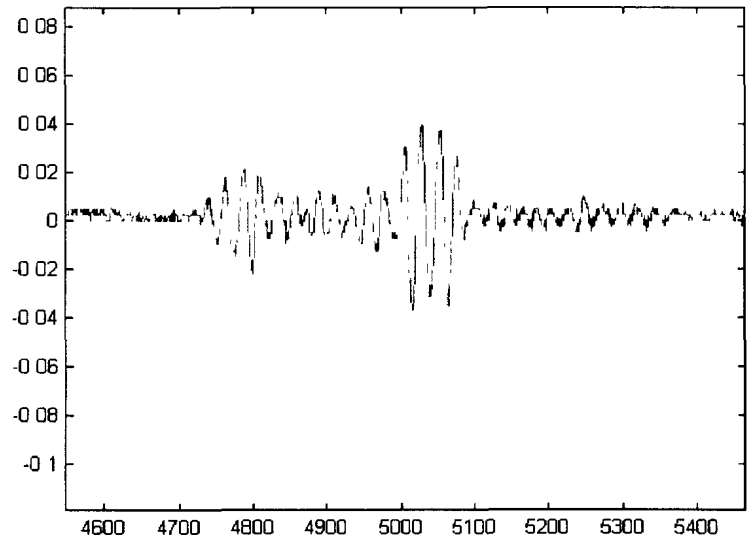

Figure 27 Backscattered 40-kHz signal from syntatic foam sphere

Diablo retro-reflector

The diablo retro-reflector is constructed from 2 sections at slightly different orientations. Each section consists of 4 triangular reflectors. It is meant to give a strong reflection (at least at certain aspects). It has been used in the past as effective marker near the seabed for sidescan sonar trials. In this experiment it was attached to the rotator pole horizontally as shown below in Fig.28. In Fig.29 the retro-reflector is shown vertically which would be the normal orientation in a sea-deployment; the individual corner reflectors can be seen in this picture. In Fig.30 the time/azimuth of the amplitude(dB) of the backscattered signal is shown; it can be seen that the retro-reflector scatters into a narrow beam centred at approximately 80 degrees (90 degrees represents the axis of the reflector horizontal to the incident energy). There is some evidence of multiple arrivals from the different portions of the reflector. This is more evident in Fig.31 which shows three of the time series in detail. It should be noted that in sidescan sonar trials this reflector is usually mounted so that its vertical axis (which is oriented horizontally here) is vertical (as in Fig.29) and the 80 degrees aspect would correspond to a grazing angle of 10 degrees. The other angle of interest is the aspect around this vertical axis. This variation has not been measured here.

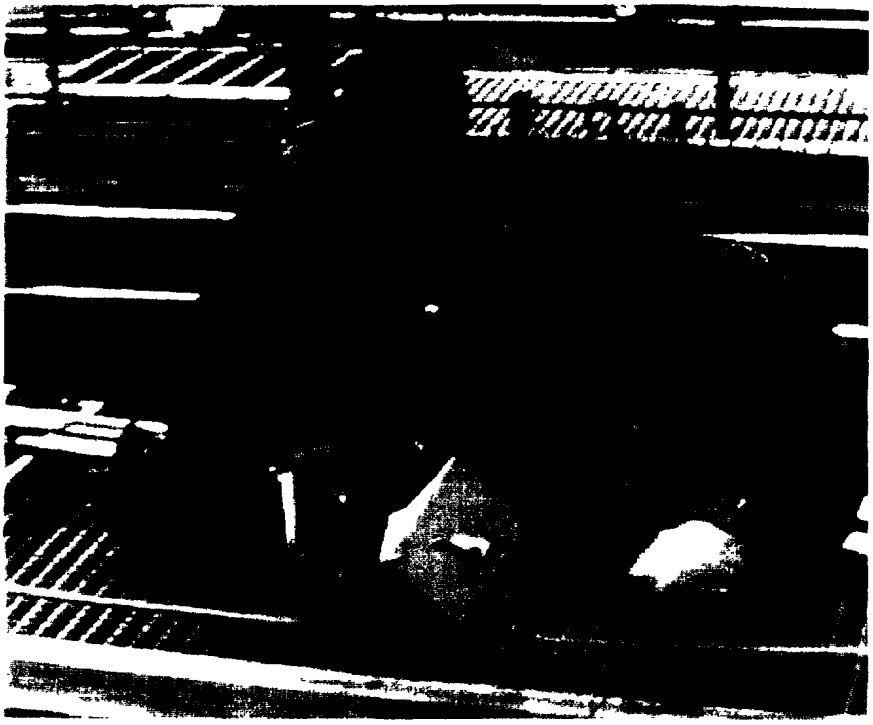

Figure 28 Mark Rowsome and Ron Kessel with retro-reflector

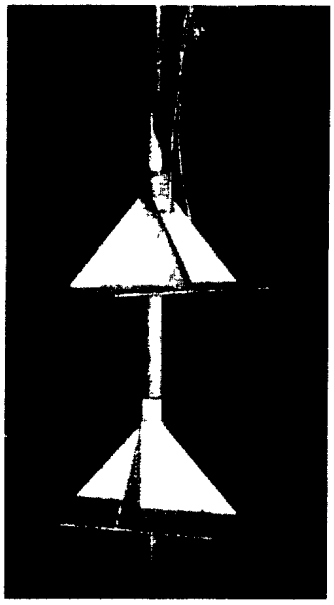

Figure 29 Vertical orientation showing 4 corner reflectors for each section

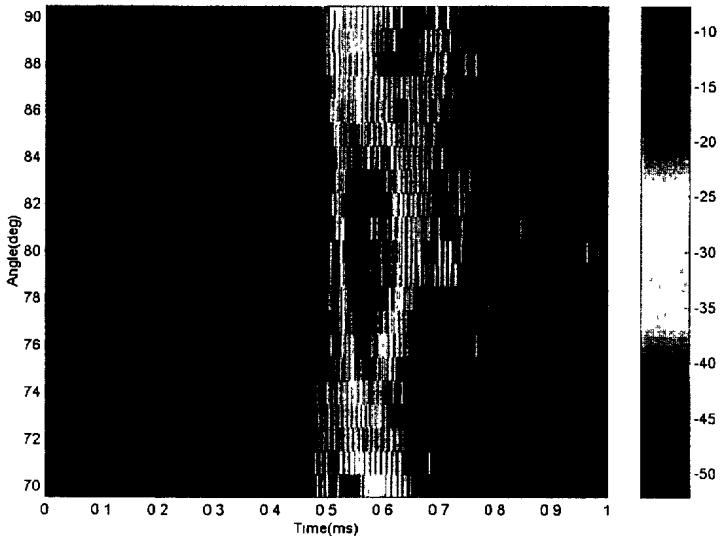

Figure 30 Time/azimuth plot for 50-kHz signal backscattered by retro-reflector

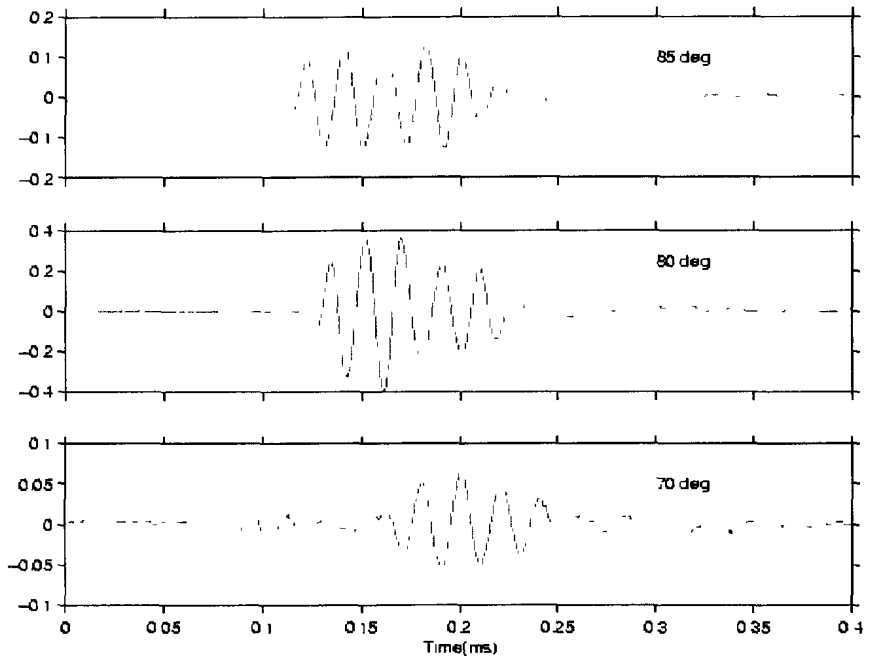

Figure 31 Variation of backscattered signal with respect to aspect

SUMMARY

In this report several interesting results have been shown for a variety of targets. All targets, with the exception of the steel-shelled sphere (theory predicts that interesting effects should start in the 100+ KHz range), exhibited some significant non-specular returns within some frequency range. For example, for the air-filled cylinder there was significant "ringing" at 10-kHz. For the same cylinder, water-filled then 30-kHz seemed to be a near-optimal frequency for non-specular returns. The rock exhibited almost a continuum of scattering from its various facets. The plate exhibited secondary arrivals; for the plate the target strength seemed to vary significantly with frequency; this was well-explained by taking the near-field effects into account. The syntatic foam sphere exhibited a non-specular return which we are presently at a loss to explain. The retro-reflector produced a narrow beam of scattered energy and the details of the scattered pulse depended significantly on aspect.

The cylinders and rock displayed strong azimuthal dependence; it was found that, in particular, for the rock that a backprojection of the scattered energy produced a very good outline of the rock's shape and reflectivity.

For the sphere and cylinder, where analytical models were possible it was found that the model/data agreement was good. In particular, for the water-filled case, the non-specular arrivals and their frequency dependence was well predicted by the Fouier-Bessel series.

In future we would like to continue this work. In particular, we have acquired a recording system capable of digitizing at 10-Mhz allowing us to capture high frequency returns. We would like to examine the scattered signals from mine-like objects on the seabed obtained from real sonar transducers, such as the various Klein transducers (100, 300 and 455 kHz) which we possess. It may be possible to combine this scattering information as additional classification information in combination with the standard highlight/shadow data or it may be that a system capable of lower frequencies is required to obtain useful scattering information.

References

1. F.D. Cotaras, "Some measurements of target strength at 20-50 kHz", DREA Note No. UA/90/5, 1991.

2. W.L.J. Fox, J.A. Fawcett, D. Jourdain-Albonico, A. Tesei, "Measurements of free-field scattering from cylindrical shells", SACLANTCEN Memorandum SM-331, 1997.

3. B. Zerr, B.Stage, "A method for the three-dimensional reconstruction of underwater objects", SACLANTCEN Memorandum SM-310, 1996.

4. B. Zerr, A. Tesei, A. Maguer, W.L.J. Fox, J.A. Fawcett "A classification technique combining aspect dependence and elastic properties of target scattering", SACLANTCEN Report SR-310, 1999.

5. R.J. Bobber, "Underwater Electroacoustic measurements",Peninsula Publishing, 1988.

6. J.A. Fawcett, "Modelling of high-frequency scattering from elastic spheres", DREA Technical Memorandum 98/233, 1999.

7. R.J. Urick, *Principles of Underwater Sound,* 3rd Edition, McGraw-Hill, 1983.

UNCLASSIFIED
SECURITY CLASSIFICATION OF FORM
(highest classification of Title, Abstract, Keywords)

DOCUMENT CONTROL DATA

(Security classification of title, body of abstract and indexing annotation must be entered when the overall document is classified)

1 ORIGINATOR (the name and address of the organization preparing the document Organizations for whom the document was prepared, e g Establishment sponsoring a contractor's report, or tasking agency, are entered in section 8)

Defence Research Establishment Atlantic
PO Box 1012
Dartmouth, Nova Scotia, Canada B2Y 3Z7

2 SECURITY CLASSIFICATION (overall security classification of the document including special warning terms if applicable)

UNCLASSIFIED

3 TITLE (the complete document title as indicated on the title page Its classification should be indicated by the appropriate abbreviation (S,C,R or U) in parentheses after the title)

Preliminary Analysis of Echo 2000 Data

4 AUTHORS (Last name, first name, middle initial If military, show rank, e g Doe, Maj John E)

John Fawcett, Ron Kessel ,Terry Miller, Vincent Myers, Mark Rowsome

5 DATE OF PUBLICATION (month and year of publication of document)	6a NO OF PAGES (total containing information Include Annexes, Appendices, etc)	6b NO OF REFS (total cited in document)
February 17, 2001	30 (approx.)	7

7 DESCRIPTIVE NOTES (the category of the document, e g technical report, technical note or memorandum If appropriate, enter the type of report, e g interim progress, summary, annual or final Give the inclusive dates when a specific reporting period is covered)

TECHNICAL MEMORANDUM

8 SPONSORING ACTIVITY (the name of the department project office or laboratory sponsoring the research and development Include address)

Defence Research Establishment Atlantic

9a PROJECT OR GRANT NO (if appropriate, the applicable research and development project or grant number under which the document was written Please specify whether project or grant)	9b CONTRACT NO (if appropriate, the applicable number under which the document was written)
Project 1da12	

10a ORIGINATOR'S DOCUMENT NUMBER (the official document number by which the document is identified by the originating activity This number must be unique to this document)	10b OTHER DOCUMENT NOs (Any other numbers which may be assigned this document either by the originator or by the sponsor)
DREA TM 2001-009	

11 DOCUMENT AVAILABILITY (any limitations on further dissemination of the document, other than those imposed by security classification)

(X) Unlimited distribution
( ) Defence departments and defence contractors; further distribution only as approved
( ) Defence departments and Canadian defence contractors; further distribution only as approved
( ) Government departments and agencies; further distribution only as approved
( ) Defence departments, further distribution only as approved
( ) Other (please specify):

12 DOCUMENT ANNOUNCEMENT (any limitation to the bibliographic announcement of this document This will normally correspond to the Document Availability (11) However, where further distribution (beyond the audience specified in (11) is possible, a wider announcement audience may be selected)

UNCLASSIFIED
SECURITY CLASSIFICATION OF FORM

UNCLASSIFIED
SECURITY CLASSIFICATION OF FORM
(highest classification of Title, Abstract, Keywords)

13. ABSTRACT (a brief and factual summary of the document It may also appear elsewhere in the body of the document itself It is highly desirable that the abstract of classified documents be unclassified Each paragraph of the abstract shall begin with an indication of the security classification of the information in the paragraph (unless the document itself is unclassified) represented as (S), (C), (R), or (U) It is not necessary to include here abstracts in both official languages unless the text is bilingual)

In this report some preliminary results from target scattering measurements made at the DREA barge in April 2000 are presented. Various targets were mounted on a pole at about 5m distance from a transducer/hydrophone arrangement. The transducer allowed for the generation of harmonic bursts in the 10-100 kHz range and the scattered signals received at the hydrophone were recorded. This data was collected for a plate, spheres, cylinders, and a rock for a variety of centre frequencies and azimuthal orientations of the targets. A very large amount of data was collected and it is not possible to give a comprehensive presentation of the data; instead an interesting sampling of some of the results of our analysis of the data are presented.

14. KEYWORDS, DESCRIPTORS or IDENTIFIERS (technically meaningful terms or short phrases that characterize a document and could be helpful in cataloguing the document They should be selected so that no security classification is required Identifiers, such as equipment model designation, trade name, military project code name, geographic location may also be included If possible keywords should be selected from a published thesaurus e g Thesaurus of Engineering and Scientific Terms (TEST) and that thesaurus-identified If it not possible to select indexing terms which are Unclassified, the classification of each should be indicated as with the title)

Scattering, sphere, cylinder

UNCLASSIFIED
SECURITY CLASSIFICATION OF FORM

Defence R&D Canada
is the national authority for providing
Science and Technology (S&T) leadership
in the advancement and maintenance
of Canada's defence capabilities.

R et D pour la défense Canada
est responsable, au niveau national, pour
les sciences et la technologie (S et T)
au service de l'avancement et du maintien des
capacités de défense du Canada.

DEFENCE R&D DÉFENSE

www.drdc-rddc.dnd.ca